

Isotropic reorientations of fullerene C₇₀ triplet molecules in solid glassy matrices revealed by light-induced electron paramagnetic resonance

Mikhail N. Uvarov,¹ Leonid V. Kulik,¹ Alexander B. Doktorov,^{1,2} and Sergei A. Dzuba^{1,2,a)}

¹*Institute of Chemical Kinetics and Combustion, Russian Academy of Sciences, Institutskaya 3, Novosibirsk 630090, Russia*

²*Novosibirsk State University, Pirogova 2, Novosibirsk 630090, Russia*

(Received 8 May 2011; accepted 8 July 2011; published online 2 August 2011)

Continuous-wave X-band electron paramagnetic resonance (EPR) of fullerene C₇₀ molecules excited to a triplet state by continuous light illumination was studied in molecular glasses of *o*-terphenyl and *cis/trans*-decalin and in the glassy polymers polymethylmethacrylate (PMMA) and polystyrene (PS). Above ~ 100 K, a distinct narrowing of EPR lineshape of the triplet was observed, which was very similar for all systems studied. EPR lineshape was simulated reasonably well within a framework of a simple model of random jumps, which implies that the C₇₀ molecule performs isotropic orientational motion by sudden jumps of arbitrary angles. In simulations, a single correlation time τ_c was used, varying in the range of 10^{-7} – 10^{-8} s. Near and below 100 K electron spin echo (ESE) signals were also obtained which were found to decay exponentially. Correlation times τ_c obtained from simulation of the EPR spectra in the slow-motion limit (τ_c close to 10^{-7} s) turned out to be in good agreement with the phase memory times T_M of the ESE decay, which additionally supports the employed simple model. The observed motional effects provide evidence that the nanostructure of the solid glassy media of different origins is soft enough to allow a large asymmetric C₇₀ molecule to reorient rapidly. Except for the EPR spectra of the triplet, in the center of the spectra, a small admixture of a narrow line was also observed; its possible nature is briefly discussed. © 2011 American Institute of Physics. [doi:10.1063/1.3618738]

I. INTRODUCTION

Orientational motion of molecular probes in glassy matrices may reflect important properties of molecular dynamics in these materials. It has been studied using different experimental approaches, such as optical depolarization,^{1–3} photobleaching,^{4,5} dielectric relaxation,⁶ nuclear magnetic resonance (NMR),^{7,8} single-molecule spectroscopy,^{9–12} and others. The dynamics of molecular probes is known to be characterized by a broad distribution of correlation times. Near the glass transition temperature, T_g , the characteristic correlation time, τ_c , of the molecular motions attains values of seconds and minutes that matches macroscopic relaxation determined by viscosity.^{1–12} It is known that the larger the probe molecule, the closer the temperature dependence of τ_c and viscosity.^{1,2,5,7}

It was also found a long time ago that highly-symmetric probe molecules experience rapid reorientations in glassy matrices, with $\tau_c < 10^{-6}$ s, at temperatures well below T_g . NMR data for axially-symmetric benzene¹³ and hexamethylbenzene^{13–15} molecules show uniaxial fast rotation, while fast motion was found to be isotropic for highly symmetric adamantane¹³ and tetramethylsilane.¹⁶

In this paper, we report fast reorientations in glassy media of a fullerene C₇₀ probe molecule. This probe is remarkably larger than those used in the above studies. Although the C₇₀ molecule is nearly spherical, it shows a noticeable

axial anisotropy. Unexpectedly, we found that in glasses the C₇₀ molecule manifests isotropic reorientations on the sub-microsecond timescale well below T_g .

We studied electron paramagnetic resonance (EPR) spectra of the photoexcited triplet state, ³C₇₀, using continuous light illumination and conventional continuous-wave (CW) X-band EPR (light-induced EPR, or LEPR). Relaxation times were obtained with the electron spin echo (ESE) technique. We used four host glassy matrices: *o*-terphenyl ($T_g = 243$ K), *cis/trans*-decalin ($T_g = 137$ K), polymethylmethacrylate (PMMA, $T_g = 378$ K), and polystyrene (PS, $T_g = 368$ K).

EPR spectra obtained under continuous light illumination of photoexcited ³C₇₀ were also presented in an earlier work,¹⁷ in which a glassy methylcyclohexane matrix was used as a host. That study found a narrowing of the EPR lineshape with temperature increase, which was ascribed to fast reorientations of C₇₀. However, this effect was discussed only qualitatively in that work. Because, the temperature range explored in that work was remarkably higher than T_g , the found motions were ascribed to a trivial effect of matrix softening.

II. EXPERIMENT

Fullerene C₇₀ of 99% purity was obtained from Aldrich. To prepare samples of fullerene in decalin (1:1 mixture of *cis*- and *trans*-decalin, Sigma-Aldrich) and in *o*-terphenyl (Tokyo, Kasei), fullerene was dissolved in these solvents at concentrations near 3×10^{-4} M (5×10^{-2} wt. %). Then samples were

^{a)} Author to whom correspondence should be addressed. Electronic mail: dzuba@kinetics.nsc.ru.

put in quartz tubes of 4.6 mm outer diameter and frozen in liquid nitrogen to obtain transparent glasses.

Four types of polymer matrices were used as host matrices for C_{70} : PMMA of average molecular weight $M_w \sim 996\,000$, PMMA of average $M_w \sim 15\,000$, PS of average $M_w \sim 350\,000$, and PS of average $M_w \sim 35\,000$ (all from Aldrich). Fullerene and polymer were taken at the proportion in which C_{70} content was near 5×10^{-2} wt.% and were initially dissolved in toluene. Then, the solution was smeared onto a glass substrate, and the toluene was evaporated initially at atmospheric pressure and then at $\sim 10^{-2}$ Torr for several hours. The resulting blend looked like a transparent film of about $100\ \mu\text{m}$ thickness.

EPR measurements were carried out with an X-band ELEXSYS ESP-580E EPR spectrometer (Bruker), which was operated either in CW or pulsed mode. In CW measurements, we used either an ELEXSYS super high sensitivity probehead cavity equipped with an ER 4131VT temperature setting device or a critically coupled ER 4118 X-MD-5 dielectric cavity inside an Oxford Instruments CF 935 cryostat. Microwave power in CW EPR was adjusted to a value low enough to avoid saturation effects; its value was less than 6.3 mW. The magnetic field modulation frequency was 100 kHz, and its amplitude was set to 1 G.

In pulsed mode, we used an overcoupled ER 4118 X-MD-5 dielectric cavity inside an Oxford Instruments CF 935 cryostat. An ESE signal was obtained using sequential microwave $\pi/2$ and π pulses, which were of 16 ns and 32 ns length, respectively. The shortest delay τ between pulses was 120 ns.

To suppress slight dark signals in CW EPR experiments, EPR spectra obtained in the dark were subtracted from light-induced EPR spectra. No dark signal was detected in the pulse EPR experiments.

Samples were continuously irradiated with light from a Xe lamp equipped with a filter transmitting light in the range between 350 nm and 700 nm. The estimated light power reaching the sample was about 10 mW.

Temperature was maintained by cold nitrogen or helium gas flow and monitored with a copper-constantan thermocouple attached to the sample.

III. RESULTS

Experimental EPR spectra of $^3C_{70}$ taken at different temperatures are shown in Fig. 1 for the decalin matrix, in Fig. 2 for the *o*-terphenyl matrix, in Fig. 3 for the PMMA matrix (average $M_w \sim 996\,000$), and in Fig. 4 for the PS matrix (average $M_w \sim 350\,000$). EPR spectra for the two other samples – PMMA, average $M_w \sim 15\,000$, and PS, average $M_w \sim 35\,000$, did not differ from the spectra of their high-molecular-weight analogs. Below 50 K spectra were found to show absorption/emissive character, due to spin polarization effect.¹⁸ Spectra in Figs. 1–4 consist of a broad line, of about 100 G width, and of a central narrow one. The integral contribution of the narrow line, estimated from double integration of EPR spectra, varies in the range between 0.1% and 10% – see Fig. 5.

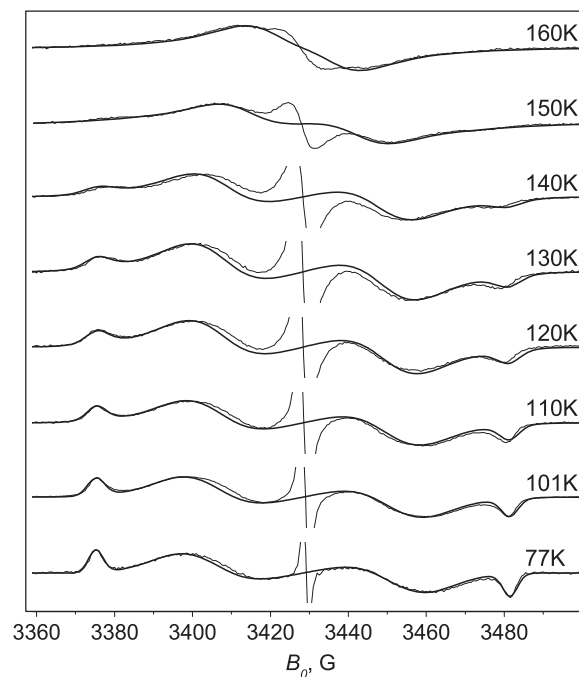


FIG. 1. EPR spectra of $^3C_{70}$ in the glassy decalin matrix at different temperatures (noisy curves) and numerical simulations based on Eq. (9) (smooth curves). Amplification is set to match the intensity of the broad line.

The broad line may be unambiguously assigned to a photoexcited triplet state, $^3C_{70}$. The shoulders, well-resolved at 77 K at both sides of the spectrum, belong to the Z canonical orientation, when the axis of axial symmetry of the molecule is directed along the external magnetic field. The broad line becomes narrower and the outer shoulders diminish with increasing temperature. This behavior may be readily assigned to the reorientation of the molecule. Although the C_{70}

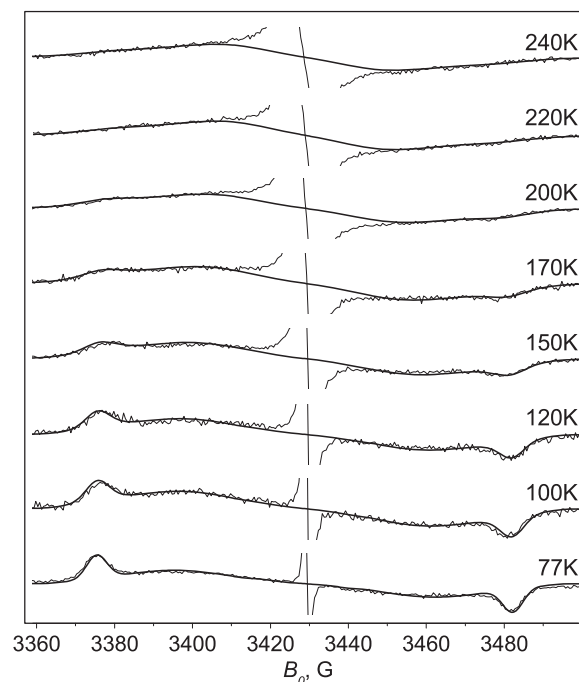


FIG. 2. The same as in Fig. 1, for glassy *o*-terphenyl matrix.

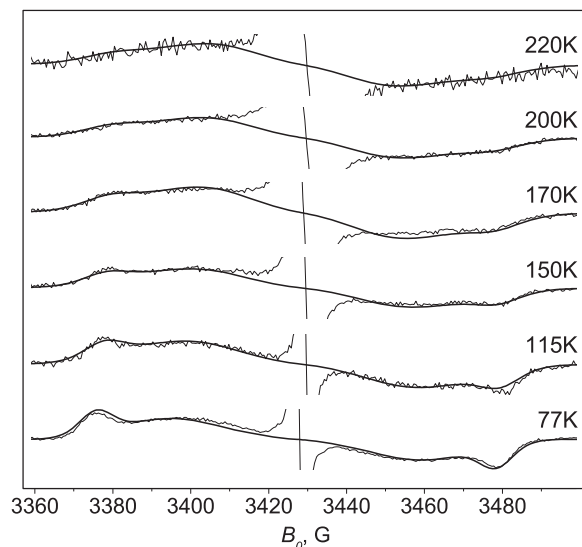


FIG. 3. The same as in Fig. 1, for PMMA (average $M_w \sim 996\,000$) matrix.

molecule possesses a preferred axis of rotation directed along the Z molecular axis, the reorientations must be isotropic for the sharp outer shoulders to disappear. The well-known pseudorotation of the excited triplet state^{19–22} cannot explain these spectral changes, because pseudorotation occurs around the Z molecular axis, which would not influence the outer shoulders. So, these changes likely reflect a physical reorientation of the molecule.

The narrow line in the center of the EPR spectrum was observed previously for a similar system¹⁷ and was interpreted as belonging to a portion of a triplet spectrum averaged by fast molecular rotation. However, this interpretation is questionable because it requires a very high rate of rota-

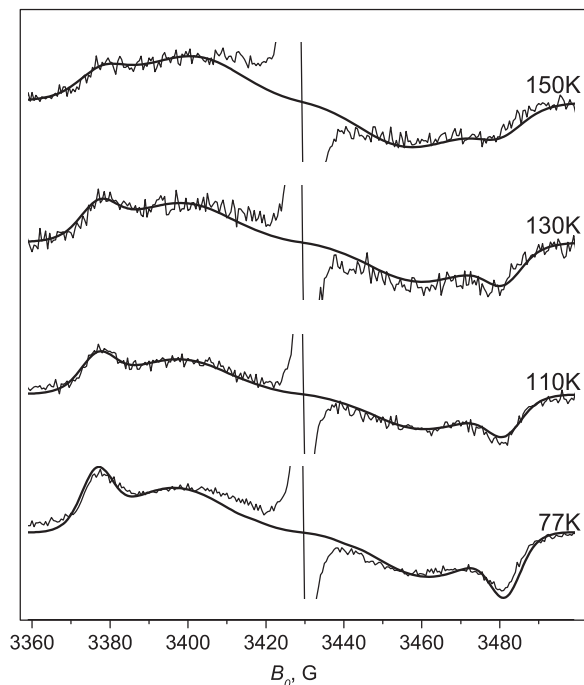


FIG. 4. The same as in Fig. 1, for PS (average $M_w \sim 350\,000$) matrix.

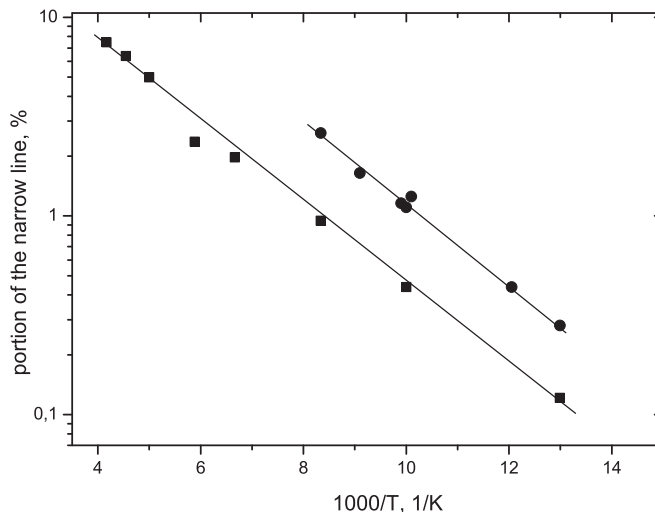


FIG. 5. The portion of EPR transitions contributing to the narrow line for $^{13}\text{C}_{70}$ in glassy *o*-terphenyl (squares) and decalin (circles) matrices.

tion, around 10^{11} s^{-1} . Such rates for C₇₀ reorientation are known only in low-viscosity aromatic solvents near the room temperature.²³ The other possible explanation is that the narrow line is associated with a C₇₀ anion radical.²⁴ As both of these explanations consider the broad and narrow lines separately, at present, we focus only on the broad line. (For this reason the vertical scales in Figs. 1–4 are enhanced.)

Transverse spin relaxation rates of $^{13}\text{C}_{70}$ were extracted from ESE decays with increasing delay τ between two pulses, at the field position at the left outer shoulder (see Figs. 1–4) of the EPR spectra. Examples of experimental traces are shown in Fig. 6 in semilogarithmic coordinates. One can see that decays are fitted satisfactorily by an exponential function. The fitting parameter was assigned to the phase memory time, T_M . (Note also slight oscillations on the ESE decay. They occur with Larmor frequency of the ^{13}C nuclei in the magnetic field applied and on that ground may be unambiguously assigned to ESE envelope modulation phenomenon.²⁶)

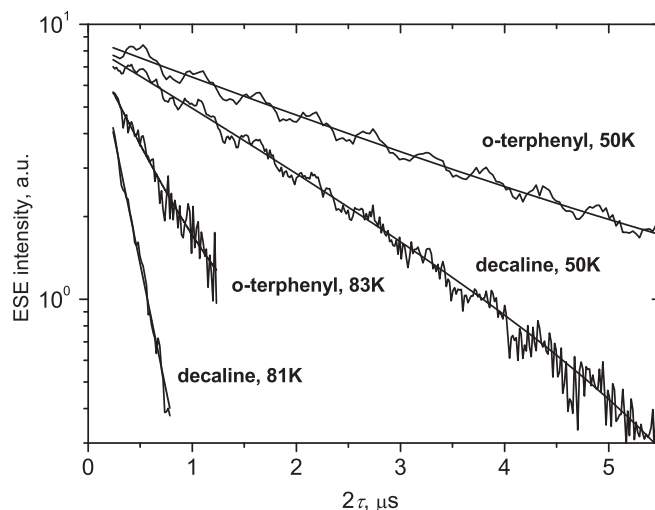


FIG. 6. Typical $^{13}\text{C}_{70}$ ESE decays in semilogarithmic coordinates. The straight lines present linear approximations, their slopes are ascribed to the reciprocal values of phase memory times T_M .

Temperature dependences of the T_M^{-1} values found in different matrices are presented in Fig. 7 as open symbols. Previously, decays of $^3\text{C}_{70}$ in decalin and *o*-terphenyl were obtained after excitation by a laser pulse;²⁵ these data are also given in Fig. 7 (as triangles). One can see that both types of experiment provide similar results.

IV. NUMERICAL SIMULATIONS OF EPR SPECTRA

If we suppose a Boltzmann distribution of spin populations for the spin sublevels, then the EPR absorption lineshape is given by²⁷

$$g(\omega) = \frac{1}{2\pi} \text{Re} \int_0^\infty \exp(-i\omega t) G(t) dt, \quad (1)$$

where ω is the microwave field frequency, and

$$G(t) = \sqrt{2} \text{Tr} \langle S_x \sigma(t) \rangle, \quad (2)$$

is an autocorrelation function. Here, S_x is the component of the spin operator (spin value is assumed to be equal to 1), and

$$\sigma(t) = \frac{1}{\sqrt{2}} \exp\left(-\frac{i}{\hbar} \mathcal{H}t\right) S_x \exp\left(\frac{i}{\hbar} \mathcal{H}t\right), \quad (3)$$

is the time-dependent density matrix ($\sigma(0) = (1/\sqrt{2})S_x$). In Eq. (2), angular brackets mean averaging over stochastic variables of the spin Hamiltonian \mathcal{H} .

In the first-order perturbation theory, the spin Hamiltonian for $^3\text{C}_{70}$ at X-band EPR may be written in the laboratory frame as²⁸

$$\mathcal{H} = g\beta \left(B_0 S_z + \frac{1}{2} \left(\frac{D}{3} (3 \cos^2 \theta - 1) + E \sin^2 \theta \cos 2\varphi \right) (3S_z^2 - \mathbf{S}^2) \right), \quad (4)$$

where B_0 is the external magnetic field, β is the Bohr magneton, g is the g -factor (assumed here to be isotropic and equal to 2.0029), D and E are dipole-dipole interaction parameters expressed in magnetic field units, and θ and φ are the polar and azimuthal angles, respectively, determining the orientation of the external magnetic field in the molecular frame. In our case $B_0 \gg D, E$, so spin is quantized along the external magnetic field, and the three spin sublevels are eigenfunctions of the Zeeman Hamiltonian, T_+ , T_0 , and T_- .

The non-zero matrix elements of S_x are

$$\begin{aligned} \langle T_0 | S_x | T_+ \rangle &= \langle T_+ | S_x | T_0 \rangle = \langle T_- | S_x | T_0 \rangle \\ &= \langle T_0 | S_x | T_- \rangle = \frac{1}{\sqrt{2}}. \end{aligned} \quad (5)$$

Because linewidth (in frequency units) is much smaller than the Zeeman frequency γB_0 , we obtain from Eqs. (1) and (2)

$$g(\omega) = \frac{1}{\pi} \text{Re} \int_0^\infty \exp(-i\omega t) (\sigma_{T_0 T_+}(t) + \sigma_{T_- T_0}(t)) dt. \quad (6)$$

The density matrix elements $\sigma_{T_0 T_+}$ and $\sigma_{T_- T_0}$ correspond to the $T_0 \leftrightarrow T_+$ and $T_0 \leftrightarrow T_-$ transitions between the adjacent triplet spin sublevels, respectively. Equation (6) implies that the time evolution of $\sigma_{T_0 T_+}$ and $\sigma_{T_- T_0}$ may be considered separately. The initial conditions are $\sigma_{T_0 T_+}(0) = \sigma_{T_- T_0}(0) = 1/2$.

The two resonance magnetic field values for the transitions, $T_0 \leftrightarrow T_+$ and $T_0 \leftrightarrow T_-$, are derived from the Hamiltonian (4) as

$$\begin{aligned} B^+ &= B_0 + \frac{D}{2} (3 \cos^2 \theta - 1) + \frac{3E}{2} \sin^2 \theta \cos 2\varphi, \\ B^- &= B_0 - \frac{D}{2} (3 \cos^2 \theta - 1) - \frac{3E}{2} \sin^2 \theta \cos 2\varphi. \end{aligned} \quad (7)$$

Recent precise analysis of the $^3\text{C}_{70}$ EPR lineshape²⁹ has showed that D and E values are distributed. D was taken to be distributed by Gaussian probability, $W_D(D) \sim \exp(-2(D - D_0)^2/(\Delta D)^2)$, while the distribution of E was determined by an empirical probability density function in the form of $W_E(E) \sim E \cdot \exp(-E^2/E_0^2)$. These distribution functions were also used in our simulations (see Ref. 29 for values of the parameters D_0 , ΔD , and E in each matrix). For comparison with experimental EPR spectra, we consider below that ω is fixed and the magnetic field B_0 is scanned.

We assumed EPR spectra to be immobilized at 77 K and performed numerical simulation by averaging the two subsystems with the resonance field positions (7) over the angles θ and φ . We assumed a Gaussian form for the individual line broadening $f(B)$ with peak-to-peak linewidth of 3 G:

$$\begin{aligned} g_\pm(B_0) &= \frac{1}{4\pi} \int W_D(D) dD \int W_E(E) dE \\ &\times \iint f\left(\frac{\omega}{\gamma} - B^\pm\right) \sin \theta d\theta d\varphi. \end{aligned} \quad (8)$$

(See Ref. 29 for further details.) The final spectra were calculated as a sum $G(B_0) = 1/2 (g_+(B_0) + g_-(B_0))$. Figures 1–4 present results of the simulations as smooth lines.

Simulations at temperatures higher than 77 K were performed using a simple model of exchange by uncorrelated jumps between all spectral positions. Since spin evolution proceeds separately in two two-level subsystems (see Eq. (6)), we consider these jumps to occur independently in two spectral subsets (transitions $T_0 \leftrightarrow T_+$ and $T_0 \leftrightarrow T_-$). In our model, we dissected the immobilized EPR spectrum (8) on an infinite number of portions characterized by a scanning magnetic field B_s^\pm , where subscript s denotes the sequential number of the portion. The probability of a resonance frequency jump from a given resonance field position was taken as τ_c^{-1} , and we assumed the probability of acquiring a new position to be proportional to the spectral intensity at this position. So, the total probability had the form $g_\pm(B_s^\pm) \tau_c^{-1}$. This model implies that exchange occurs due to orientational motion of the molecule by uncorrelated isotropic angular jumps, which modulates angles θ and φ in Eq. (7).

In this simple model, one can readily get the lineshape by applying modified Bloch equations (or a stochastic Liouville equation for the density matrix) for uncorrelated spectral diffusion within two independent two-level subsets:³⁰

$$G_\pm(B_0) = T_2 \text{Re} \left[\frac{\frac{1}{\pi} \sum_s \frac{g_\pm(B_s^\pm)}{1 + \tau_c T_2^{-1} + i\gamma(B_0 - B_s^\pm)\tau_c}}{\sum_s g_\pm(B_s^\pm) \frac{1 + i\gamma(B_0 - B_s^\pm)T_2}{1 + \tau_c T_2^{-1} + i\gamma(B_0 - B_s^\pm)\tau_c}} \right]. \quad (9)$$

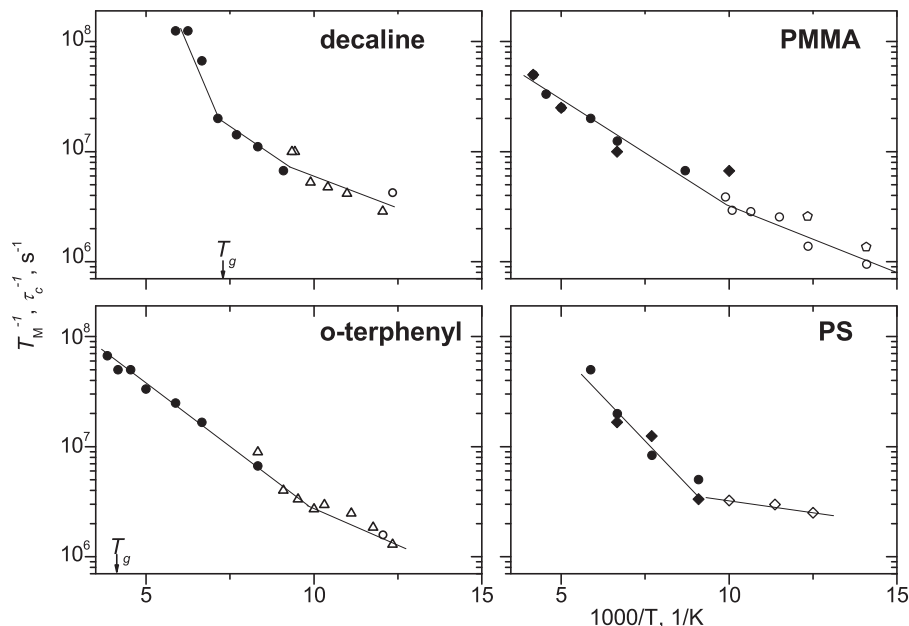


FIG. 7. Temperature dependences of reciprocal values of phase memory times T_M obtained from ESE decays (open symbols) and correlation times τ_c obtained from numerical simulation of EPR spectra (filled symbols), for $^3\text{C}_{70}$ in different glassy matrices. For decalin and *o*-terphenyl, ESE data given by triangles are taken from Ref. 25. For PMMA, circles refer to average $M_w \sim 996\,000$, and rhombs to average $M_w \sim 15\,000$. For PS, circles refer to average $M_w \sim 350\,000$, and rhombs refer to average $M_w \sim 35\,000$. For decalin and *o*-terphenyl, glass transition temperature T_g is indicated. The lines are drawn to guide the eye.

The intrinsic relaxation time T_2 , which is not associated with molecular motion, is assumed here to be independent of index s . T_2 was taken as $5\ \mu\text{s}$ for all cases in simulations. The final simulated temperature-dependent EPR spectra were taken as a sum, $G(B_0) = 1/2(G_+(B_0) + G_-(B_0))$ and were averaged in the same way as in Eq. (8). The τ_c value was the only fitting parameter in comparison with experimental spectra at elevated temperatures. Figures 1–4 show the simulation results with smooth lines as first derivatives $dG(B_0)/dB_0$. One can see quite a good agreement between experiment and simulation at all temperatures for all systems studied. The filled symbols in the Arrhenius plot of Fig. 7 show temperature dependences of the best-fitted τ_c^{-1} values.

V. DISCUSSION

Our EPR spectra of photoexcited fullerene C₇₀ triplet molecules in solid glassy matrices show a noticeable narrowing with increase of temperature. This narrowing is described fairly well by a simple model of random walks within the EPR lineshape, which implies that molecules undergo isotropic reorientations by uncorrelated angular jumps (Figs. 1–4). Surprisingly, we found a single correlation time τ_c to be enough to describe the experimental spectra fairly well (a broad distribution of correlation times is often required to describe dynamical properties of glassy media).

Values of τ_c extracted from EPR spectral simulations agree well with ESE data on the T_M phase memory time at temperatures where both techniques may be applied. This additionally supports the model of uncorrelated jumps, because $T_M = \tau_c$ for this model in the case of slow motions (when the total narrowing does not yet appear, i.e., when $\gamma D\tau_c \gg 1$). Note that ESE is more sensitive to slower

motions than CW EPR, because in the former case inhomogeneous line broadening is eliminated.

Also note that the observed exponential ESE decays (Fig. 6) support the above conclusion that correlation time τ_c is not distributed in our case.

Reorientations of a large fullerene C₇₀ molecule occur many orders of magnitude faster than is known for other probe molecules in molecular glasses.^{1–12} An exception is the case of highly-symmetric probe molecules—benzene,¹³ hexamethylbenzene,^{14,15} tetramethylsilane,¹⁶ and adamantane,¹³ for which NMR data also indicate fast rotations, with $\tau_c < 10^{-6}$ s. (In some cases, it was also reported that EPR of nitroxide spin labels in molecular glasses and polymeric systems showed fast reorientations, but this interpretation seems to be incorrect⁶). The other important common feature between fullerene C₇₀ and these symmetric molecules is that rotations in all cases appear approximately in the same temperature range, close to ~ 100 K.

High symmetry is important for fast motion, because for tetramethylsilane¹⁶ and adamantane¹³ (tetrahedral symmetry group, T_d) the motion is isotropic while for axially symmetric benzene¹³ and hexamethylbenzene^{13–15} (D_{6h} symmetry) it is uniaxial. In that respect, it must be noted that although the C₇₀ molecule is nearly spherical, it has noticeable axial anisotropy (the D_{5h} symmetry group). The longest dimension of the C₇₀ carbon skeleton is equal to 0.79 nm, and the equatorial dimension is equal to 0.72 nm.³¹ Upon photoexcitation into the triplet state, the symmetry becomes even lower due to Jahn-Teller distortions. However, these distortions are relatively small.³²

Except for the broad triplet line, we also detected a narrow line in the center of the spectrum in all cases (Figs. 1–4). Its nature is still unclear. As stated above, it may be attributed to a radical anion C_{70}^- , or to a small fraction of $^3\text{C}_{70}$ molecules

experiencing fast rotation (τ_c in a picoseconds time region) characteristic of liquid solutions of low viscosity. Also, first-order perturbation theory may not describe the system properly. Anyway, the nature of the narrow line deserves further experimental and theoretical exploration. The important empirical fact that must be explained in these studies is the apparent Arrhenius temperature dependence seen in Fig. 5.

The cumulative EPR and ESE data show an apparent lowering of the activation energy with temperature decrease below 100 K (Fig. 7). This may be explained by the influence on ESE decay at low temperatures of an additional relaxation process resulting from pseudorotations,^{19–22,25} appearing because of the dynamic Jahn-Teller effect.

As the size of the C_{70} molecule is close to 1 nm, this molecule probes dynamics at nanoscale distances. We may conclude that nanostructure of glassy media well below glass transition temperature is soft enough to allow sub-microsecond reorientations of C_{70} molecular probes.

It is interesting to note in that respect that ESE studies³³ of distance distribution between D^+ and Q_A^- cofactors in photosynthetic reaction centers show that this distribution (centered around 2.9 nm) becomes much narrower above ~ 100 K that is also well below glass transition temperature for this system. This finding may also be interpreted as a result of a softness of the nanostructure.

All the systems studied here show very similar behavior regarding the temperature dependence and temperature region where motions are detected. This is irrespective of their T_g , which is very different for different systems. The only exception is decalin above ~ 140 K, where apparent activation energy becomes noticeably larger than in the other cases. This is attributable to the fact that the motion here is studied above T_g . So, the fast reorientation found for a nm-sized probe may reflect some general property of the nanostructure of disordered media.

The abnormally short correlation times and extremely weak temperature dependences found may indicate that motion of C_{70} is related to β -relaxation in molecular glasses (i.e., secondary relaxation, Johari-Goldstein relaxation).³⁴ This is also characterized by short relaxation times and weak temperature dependence compared with primary α -relaxation. However, peaks ascribed to β -relaxation in *o*-terphenyl³⁴ and decaline³⁵ glassy liquids correspond to frequencies several orders of magnitude smaller than τ_c^{-1} values presented in Fig. 7 for the same temperatures. Therefore, dielectric β -relaxation is a much slower process. Also, temperature dependences of these frequencies normally are much stronger than temperature dependences of τ_c^{-1} values observed here for reorientations of C_{70} . From the other side, peaks of dielectric β -relaxation are very broad,^{34,35} indicating a very complicated hierarchical pattern of molecular motions in glassy media. Meanwhile, reorientations of C_{70} reflect molecular motion of a selected size scale, so this may be evidence of only one selected β -relaxation pathway.

VI. CONCLUSIONS

Our results show that nm-sized fullerene C_{70} molecules reorient isotropically in solid glassy matrices. The EPR spec-

tra indicates that motion of a photoexcited triplet molecule occurs with characteristic times τ_c of 10^{-8} – 10^{-7} s. Motion is observed above ~ 100 K in the same temperature range for glassy media having essentially different glass transition temperatures: in molecular glasses of *o*-terphenyl ($T_g = 243$ K) and *cis/trans*-decalin (137 K) and in glassy polymeric matrices of PMMA (378 K) and PS (368 K). So, we may conclude that the nanostructure of glassy media is soft enough to allow fast isotropic reorientations of large C_{70} molecular probes and that this property has a universal nature for disordered media of different origin.

EPR spectra are simulated fairly well within a simple theoretical model based on modified Bloch equations independently applied to two spin transitions in the triplet. EPR data in the slow-motion limit (τ_c close to 10^{-7} s) are in good agreement with data on ESE decay, which additionally supports the suggested simple model.

The interesting feature of the observed motion is that spectral simulation does not require τ_c to be distributed over a broad range (as normally faced when studying motions below T_g – for example, by dielectric relaxation). Also, ESE decays were found to be exponential, which is in agreement with the conclusion that τ_c is not distributed.

Also, temperature dependences of τ_c were found to be very weak, even much weaker than what is known for secondary Johari-Goldstein dielectric relaxation in glasses.

ACKNOWLEDGMENTS

This work was supported by Presidium of RAS, Project No. 27.55.

- ¹M. Yang and R. Richert, *Chem. Phys.* **284**, 103 (2002).
- ²L.-M. Wang and R. Richert, *J. Chem. Phys.* **120**, 11082 (2004).
- ³S. Yu. Grebenkin and B. V. Bol'shakov, *J. Phys. Chem. B* **110**, 8582 (2006).
- ⁴P. D. Hyde, T. E. Evert, M. T. Cicerone, and M. D. Ediger, *J. Non-Cryst. Solids* **131**, 42 (1991).
- ⁵M. T. Cicerone, F. R. Blackburn, and M. D. Ediger, *J. Chem. Phys.* **102**, 471 (1995).
- ⁶W. Huang and R. Richert, *J. Chem. Phys.* **133**, 214501 (2010).
- ⁷R. Böhmer, G. Diezemann, G. Hinze, and E. Rössler, *Prog. Nucl. Magn. Reson. Spectrosc.* **39**, 191 (2001).
- ⁸P. Medick, M. Vogel, and E. Rössler, *J. Magn. Reson.* **159**, 126 (2002).
- ⁹S. A. Mackowiak, L. M. Leone, and L. J. Kaufman, *Phys. Chem. Chem. Phys.* **13**, 1786 (2011).
- ¹⁰G. Hinze, T. Basché, and R. A. L. Vallée, *Phys. Chem. Chem. Phys.* **13**, 1813 (2011).
- ¹¹I. Yu. Eremchev, Yu. G. Vainer, A. V. Naumov, and L. Kador, *Phys. Chem. Chem. Phys.* **13**, 1843 (2011).
- ¹²S. Adhikari, M. Selmke, and F. Cichos, *Phys. Chem. Chem. Phys.* **13**, 1849 (2011).
- ¹³E. Rössler, K. Börner, M. Schultz, and M. Taupitz, *J. Non-Cryst. Solids* **131–133**, 99 (1991).
- ¹⁴B. Jansen-Glaw, E. Rössler, M. Taupitz, and H. M. Vieth, *J. Chem. Phys.* **90**, 6858 (1989).
- ¹⁵E. Rössler, M. Taupitz, K. Börner, M. Schulz, and H.-M. Vieth, *J. Chem. Phys.* **92**, 5847 (1990).
- ¹⁶E. Rössler, J. Tauchert, and P. Eiermann, *J. Phys. Chem.* **98**, 8173 (1994).
- ¹⁷G. L. Closs, P. Gautam, D. Zhang, P. J. Krusi, S. A. Hill, and E. Wasserman, *J. Phys. Chem.* **96**, 5228 (1992).
- ¹⁸M. N. Uvarov, L. V. Kulik, T. I. Pichugina, and S. A. Dzuba, *Spectrochim. Acta, Part A* **78**, 1548 (2011).
- ¹⁹M. Terazima, K. Sakurada, N. Hirota, H. Shinohara, and Y. Saito, *J. Phys. Chem.* **97**, 5447 (1993).
- ²⁰G. Agostini, C. Corvaja, and L. Pasimeni, *Chem. Phys.* **202**, 349 (1996).

- ²¹H. Levanon, V. Meiklyar, S. Michaeli, and D. Gamliel, *J. Am. Chem. Soc.* **115**, 8722 (1993).
- ²²X. L. R. Dauw, O. G. Poluektov, J. B. M. Warntjes, M. V. Bronsveld, and E. J. J. Groenen, *J. Phys. Chem. A* **102**, 3078 (1998).
- ²³R. M. Hughes, P. Mutzenhardt, L. Bartolotti, and A. A. Rodriguez, *J. Phys. Chem. A* **112**, 4186 (2008).
- ²⁴M. Baumgarten and L. Gherghel, *Appl. Magn. Reson.* **11**, 171 (1996).
- ²⁵M. N. Uvarov, L. V. Kulik, and S. A. Dzuba, *J. Chem. Phys.* **131**, 144501 (2009).
- ²⁶S. A. Dikanov and Yu. D. Tsvetkov, *Electron Spin Echo Modulation (ESEEM) Spectroscopy* (CRC, Boca Raton, 1992).
- ²⁷A. Abragam, *The Principles of Nuclear Magnetism* (Clarendon, Oxford, 1961).
- ²⁸E. Wasserman, L. C. Snyder, and W. A. Yager, *J. Chem. Phys.* **41**, 1763 (1964).
- ²⁹M. N. Uvarov, L. V. Kulik, and S. A. Dzuba, "Fullerene C₇₀ triplet zero-field splitting parameters revisited by light-induced EPR at thermal equilibrium," *Appl. Magn. Reson.* (in press).
- ³⁰J. T. Arnold, *Phys. Rev.* **102**, 136 (1956).
- ³¹K. Hedberg, L. Hegberg, M. Buhl, D. S. Bethune, C. A. Brown, and R. D. Johnson, *J. Am. Chem. Soc.* **119**, 5314 (1997).
- ³²P. R. Surjan, K. Nemeth, and M. Kallay, *J. Mol. Struct.: THEOCHEM* **398**, 293 (1997).
- ³³S. A. Dzuba, P. Gast, and A. J. Hoff, *Chem. Phys. Lett.* **268**, 273 (1997).
- ³⁴G. P. Johari and M. Goldstein, *J. Chem. Phys.* **53**, 2372 (1970).
- ³⁵K. Duvvuri and R. Richert, *J. Chem. Phys.* **117**, 4414 (2002).